Research Square

Preprints are preliminary reports that have not undergone peer review.
They should not be considered conclusive, used to inform clinical practice,
or referenced by the media as validated information.

Quantifying treatment-emergent persisters reveals substantial drug-induced persistence along a tolerance spectrum

Rahul Sarpeshkar

rahul.sparpehkar@dartmouth.edu

Dartmouth College

Yijie Deng

Thayer School of Engineering

Douglas Beahm

Dartouth College https://orcid.org/0000-0002-8039-020X

Hannah Maurais

Dartouth College

Kai Etheridge

Dartouth College

Daniel Schultz

Geisel School of Medicine at Dartmouth https://orcid.org/0000-0002-3080-3416

Article

Keywords:

Posted Date: March 12th, 2026

DOI: https://doi.org/10.21203/rs.3.rs-9022969/v1

License: This work is licensed under a Creative Commons Attribution 4.0 International License.
Read Full License

Additional Declarations: There is **NO** Competing Interest.

Abstract

Antibiotics are known to induce new persister cells during treatment, yet the inability to distinguish and quantify pre-existing versus drug-induced persisters has long underestimated the extent of treatment-emergent persistence and obscured how antibiotics and genetic factors shape persistence. Here, we develop a quantitative framework integrating kinetic modeling with a novel serial-dilution time-kill (SDTK) strategy to resolve persister population dynamics and accurately quantify both persister types. We find that bactericidal antibiotics dynamically generate a substantial number of persisters that are heterogeneous and distributed along a persistence spectrum. Across antibiotics, we uncover pronounced differences in rates of persister induction and elimination, with ampicillin inducing persisters at the highest rate and kanamycin at the lowest. Depending on the dilution history, drug-induced persisters can dominate the persister pool. Our framework enables identification of drug-dependent pre-existing persister fractions and genetic determinants that differentially regulate pre-existing and/or drug-induced persistence. Using systematic sequential-drug treatments, we resolve the nested hierarchical structure among persister subsets, demonstrating that kanamycin persisters form the most tolerant subset, embedded within ciprofloxacin persisters that in turn are nested within the broader ampicillin persister subpopulation. Together, we propose a Drug-Induced Persistence-Spectrum (DIPS) model in which antibiotics differentially induce and select persister subsets along a tolerance continuum. These findings reframe persistence as stress-induced, treatment-responsive phenotypic heterogeneity and provide a unifying model with broad implications for drug tolerance and therapeutic failure in bacteria, yeasts, and cancers.

Main

The global crisis of antimicrobial resistance (AMR) is a major driver of antibiotic treatment failure [1], but non-heritable mechanisms such as antibiotic persistence also substantially undermine therapeutic efficacy, promote recurrent and chronic infections, and facilitate the evolution of antibiotic resistance [2–5]. Antibiotic persistence arises from rare phenotypically tolerant cells, called “persisters”, which survive lethal antibiotic exposure without acquiring genetic resistance. These cells typically constitute <0.1% of bacterial populations, adopt metabolically slow or dormant states, and resuscitate after drug removal [6,7].

Although a myriad of molecular pathways and stochastic mechanisms have been identified and reviewed for persister formation [2,7,16,17,8–15], their relative contributions, degree of independence, and hierarchical interactions remain widely debated. Persisters are commonly categorized as spontaneous persisters, which arise stochastically during growth and are extremely rare, and triggered persisters, which emerge in response to environmental stress and dominate the persister population [8,14].

The prevailing view of antibiotic persistence can be considered as the “pre-existing persister model,” which posits that nearly all persister cells exist before antibiotic exposure and that treatment merely reveals persisters without altering their numbers in time-kill assays [18]. However, accumulating evidence

suggests that bactericidal antibiotics themselves can promote entry into persistence [18–21]. Therefore, we propose a more general framework—the "drug-induced persister model"—in which antibiotic treatment not only reveals but also induces persisters. This new model accounts for both persisters that exist before antibiotic exposure (pre-existing persisters) and those generated during the treatment (drug-induced persisters).

Despite decades of research, the field still lacks a reliable methodology to distinguish the two persister subsets. This limitation has long prevented accurate quantification of treatment-emergent persisters and obscures how different antibiotics or genetic factors influence persister formation. Single-cell approaches yielded valuable insights into phenotypic heterogeneity and antibiotic persistence [15,22–24]. However, these techniques remain constrained by the lack of definitive biomarkers for persister cells and insufficient resolution and throughput to reliably track these extremely rare persisters. This challenge extends beyond bacterial systems to drug-persistent yeasts and drug-tolerant persister cancer cells, where surviving populations include the mixture of pre-existing persisters and cells that actively transition into tolerance during treatment [25–28]. Across biological systems, the inability to discriminate these populations has hindered efforts to characterize the dynamic formation of persisters during treatment and to determine the roles of treatment-induced molecular reprogramming in persistence development. Further, this methodological gap obstructs the development of therapeutic strategies aimed at reducing treatment-induced persistence.

Here, we address this long-standing challenge by developing a quantitative kinetic framework that integrates mathematical modeling with a newly designed serial-dilution time–kill (SDTK) assay. This quantitative approach validates the more general "drug-induced persister model" and enables direct quantification of both pre-existing and drug-induced persisters within the same culture. While drug-dependent persister fractions show substantial heterogeneity in persistence, the relationship among persister subsets across antibiotics has remained unclear. By combining this framework with systematic sequential-drug-treatment experiments, we demonstrate that persistence is a dynamic, drug-induced process that generates heterogeneous persister subsets with nested structure distributed along a spectrum of tolerance. Our findings support a drug-induced-persistence-spectrum (DIPS) model that could reshape the conceptual foundation of antibiotic persistence and provide a generalizable strategy for dissecting treatment-induced phenotypic tolerance.

Results

Experimental design and quantification of the drug-induced persisters

We establish a simple yet powerful methodology to distinguish between the pre-existing-persister and drug-induced-persister models. We integrate biphasic kinetic modeling with a new experimental strategy: the serial-dilution time-kill (SDTK) assay (Fig. 1a). In this assay, a single overnight seed culture is serially diluted (e.g., 100×, 1,000×, 10,000×) into fresh pre-warmed medium, and all resulting cultures are grown to the same optical density in exponential phase before antibiotic addition, followed by standard time-kill

measurements. The pre-existing persisters in these cultures should scale proportionally to the serial dilution factor (e.g., 10x). Fitting experimental data to mathematical models allows us to distinguish between two models, determine the key parameters, and quantify both pre-existing and drug-induced persisters (Fig. 1b).

The rationale for this approach is based on two well-established observations. First, spontaneous persisters arise at extremely low frequencies during exponential growth [8,14], making their contribution negligible relative to the persisters originating from the stationary-phase inoculum. Second, pre-existing persister cells, while metabolically active at low levels, propagate minimally in number upon reinoculation into fresh medium during early exponential growth [7,13,29,30]. Under these assumptions, the pre-existing persister model predicts that persister abundance should scale inversely with dilution: more diluted cultures contain proportionally fewer persisters, yielding evenly spaced secondary killing phases across serially diluted time–kill curves (Fig. 1b).

In contrast, the drug-induced persister model predicts a distinct and testable outcome: if antibiotics induce new persisters during treatment, then the more diluted cultures should show greater increases in relative survival because newly formed persisters constitute a larger proportion of the persister pool when the initial persister number is smaller. Thus, the divergent predictions (Fig. 1b) are uniquely resolved by the SDTK assays (see Methods for details).

We performed SDTK assays on *E. coli* treated with three classes of bactericidal antibiotics with distinct mechanisms of action: ampicillin (cell-wall synthesis inhibitor), ciprofloxacin (DNA replication inhibitor), and kanamycin (translation inhibitor). Across all three antibiotics, we observed a consistent pattern: instead of showing proportionally lower survival in serially diluted cultures (predicted by the pre-existing persister model), survival fractions were elevated with higher dilutions (Fig. 2a). Our results unambiguously demonstrates that antibiotic exposure, even at high doses (10× MIC), rapidly triggers the formation of persisters, consistent with the drug-induced persister model.

Turbidostatic experiments further validated the drug-induced persister model (Fig. 2b,c). In continuous exponential growth, persisters carried over from the stationary phase are diluted to negligible levels, such that persister cells must predominantly arise from drug-induced formation regardless of initial inoculation density. Consistent with this prediction, all dilution series yielded nearly overlapping time–kill curves (Fig. 2c). These results confirm that antibiotic exposure alone can generate a substantial number of persisters.

An alternative explanation is that more-diluted cultures undergo longer exponential growth before reaching the same optical density, potentially generating more spontaneous persisters. However, this effect is partially offset by the proportionally smaller initial population size. To conclusively rule out this possibility, we developed a quantitative model incorporating spontaneous persister formation during exponential growth based on a previous framework [14] and simulated population dynamics from inoculation through 8 h after antibiotic exposure. Spontaneous persister formation had negligible effects

on survival and failed to reproduce the SDTK patterns (Fig. S1), even when the spontaneous formation rate (a_2) was increased 100-fold above previously measured values [14] (Fig. S1f,g). A combined spontaneous and drug-induced model was similarly unnecessary (Fig. S1e). Similar results were observed in turbidostatic simulations (Fig. S2), which require biologically implausible (200–650-fold) increases in a_2 to approximate the data (Fig. S2g; Table S1). In contrast, simulations show that >99.8% of persisters arose during antibiotic exposure (Table S1), demonstrating that drug-induced persister formation alone explains the observed dynamics.

Combining kinetic modeling with SDTK experiments, we accurately quantified both pre-existing and drug-induced persisters within the same population—an otherwise extremely difficult task. Across all three antibiotics, a substantial fraction of persisters emerged during antibiotic exposure. The relative contributions of the two persister types depended strongly on the dilution factor (i.e., initial number of pre-existing persisters). Drug-induced persisters comprised ~10% of total persisters in 100-fold diluted cultures, ~50% in 1,000-fold dilutions, and >80% in 10,000-fold dilutions (Fig. 2d). Although drug-induced persisters are generated in similar absolute numbers across dilutions, their relative contribution increases at higher dilutions because the initial pre-existing persister pool size is smaller. These results demonstrate that drug-induced persisters can dominate the persister subpopulation at high seed dilutions, challenging the prevailing view that pre-existing persisters overwhelmingly dictate the persister pool.

The dynamic nature of antibiotic persistence cautions against conventional persister measurements. First, persister frequencies are time-dependent such that sampling time strongly influences apparent persister frequencies. Second, because the persister pool comprises both pre-existing and drug-induced persisters, reporting a single persister fraction without distinguishing these subsets can confound comparisons and obscure gene or stress-response functions. Third, apparent persister levels depend on dilution history, with less-diluted cultures yielding higher values, necessitating careful control across conditions. Together, these considerations underscore the need to account for persister subtype, dilution history, and timing when quantifying and comparing persistence.

The dynamics of antibiotic killing and persister formation depend on the drugs

Our framework enables quantitative, side-by-side comparisons of antibiotic efficacy against both susceptible and persister subpopulations across antibiotics (all at 10× MICs). In addition, it provides a simple and robust means to measure persister-formation rates. Using this approach, we found that the rate at which persisters emerge during treatment is strongly drug-dependent, following the order ampicillin > ciprofloxacin > kanamycin (Fig. 3a). This ranking indicates that ampicillin exposure induces persister formation more rapidly than ciprofloxacin or kanamycin exposure.

Drug efficacy varied substantially across antibiotics in their killing activity against susceptible and persister subpopulations. Although ampicillin eliminates susceptible cells more slowly than ciprofloxacin and kanamycin (Fig. 3b), it kills persister cells faster than ciprofloxacin but not kanamycin (Fig. 3c). These results illustrate that the relative potency of an antibiotic against actively growing cells does not

necessarily predict its effectiveness against persisters, emphasizing that persistence represents a distinct physiological state with drug-specific vulnerabilities.

We identified significant drug-dependent differences in pre-existing persister fractions. In exponential-phase cultures derived from a 1,000-fold diluted inoculum, the pre-existing persister fraction for ampicillin (~0.03%) was more than an order of magnitude higher than that for ciprofloxacin, which in turn was more than two orders of magnitude higher than that for kanamycin (Fig. 3d). These results indicate that persister fractions depend strongly on the antibiotic used and are therefore comparable only within assays involving the same drug; cross-antibiotic comparisons of persister abundance should be interpreted with caution.

Our findings further reveal that persisters are not the same even before antibiotic exposure and possess drug-specific survival thresholds. A cell persistent to ampicillin is not necessarily persistent to ciprofloxacin or kanamycin, indicating that persister phenotypes are not homogeneous but instead reflect various metabolic or physiological states tailored to each antibiotic class [31]. The substantially higher abundance of ampicillin persisters than ciprofloxacin or kanamycin persisters from the same culture (Fig. 3d, Fig. S4 b) indicates the possibility that ampicillin persisters are less persistent than the latter two and thus easier to form during drug exposure with higher f_1 (Fig. 3a) (more discussion below).

Dissecting gene functions in the formation of pre-existing and drug-induced persisters

Quantitative separation of pre-existing persisters from those formed during drug exposure enables the mechanistic dissection of gene functions underlying persistence—specifically, whether a gene influences the formation of pre-existing persisters, drug-induced persisters, or both. Using the SDTK approach, we measured killing kinetics, persister fractions, and persister formation rates in wild-type and mutant strains lacking key regulators of the stringent response and stress adaptation. We specifically examined whether ppGpp (synthesized by RelA and SpoT) promotes the formation of pre-existing persisters during the stationary phase and/or new persisters during antibiotic treatment, a distinction that is obscured in conventional time-kill assays. Additionally, inorganic polyphosphate (polyP) is a key regulator of bacterial metabolism and stress responses [32,33], yet its contribution to antibiotic persistence remains elusive. Therefore, we also evaluated the role of polyP, synthesized by polyphosphate kinase (PPK) in each of these processes. Representative SDTK curves for *Δppk* and *ΔrelAΔspoT* are shown in Fig. 4a,b.

Although MIC values were unchanged in the *ΔrelAΔspoT* and *Δppk* strains compared to the wild-type strain (Fig. 4c), the *ΔrelAΔspoT* mutant exhibited substantially reduced persister-formation rates during ampicillin exposure (Fig. 4d), demonstrating that ppGpp is important for the efficient generation of drug-induced persisters. Meanwhile, the *ΔrelAΔspoT* mutant produced far fewer pre-existing persisters (Fig. 4e), indicating that ppGpp also increases persister formation during the stationary phase in addition to its role in forming persisters during drug exposure. The *ΔrelAΔspoT* strain's strong defect in persister formation is consistent with the central role of ppGpp in metabolic downshifting and antibiotic persistence [10,34,35]. However, the *ΔrelAΔspoT* mutant did not abolish the formation of pre-existing[34] or

drug-induced persisters. The *Δppk* mutant consistently showed reduced persister formation rates and lower levels of pre-existing persisters compared to the wild-type strain (Fig. 4d,e), supporting a positive role for polyP in promoting antibiotic persistence, although these differences did not reach statistical significance. In addition to the altered persister dynamics, susceptible cells of both mutants appeared to be killed more rapidly (with larger k_1), although the differences were not statistically significant (Fig. 4f,g). In sum, while polyP plays a minor role in persistence, ppGpp strongly promotes persister formation during both the stationary phase and antibiotic treatment, presumably by slowing metabolism, arresting growth, and activating stress-response pathways such as the SOS and oxidative-stress responses[10,36,37], collectively protecting cells from stress-induced damage.

Dynamics of persister formation and antibiotic killing

A key advantage of our approach is that it resolves the population-level dynamics of persister formation without using specialized single-cell platforms. Analyzing cultures from 1,000-fold dilutions as an example, our model shows that new persisters emerge rapidly during the earliest phase of antibiotic exposure, typically within the first 20 minutes, regardless of antibiotics (Fig. 5a). The rapid rise in persister numbers is even more pronounced in cultures derived from 10,000-fold dilutions (Fig. S3a,b). This observation can be readily explained: pre-existing persisters are present at much lower levels in these cultures, so even a modest persister-formation rate (f_1) can generate a comparatively substantial number of new persisters from the large susceptible cell population within a small time window; as a result, newly-formed persisters quickly outnumber pre-existing persisters and dominate the persister subpopulation within 20 min (Fig. S3c). This timing is also consistent with reports that fluoroquinolones trigger immediate changes in the gene expression profile, such as the activation of SOS response and DNA repair programs within 10-25 minutes [19,38], which can drive rapid induction of persisters [19].

Population composition analysis further illustrates these dynamics (Fig. 5c). At 0.5 h, susceptible cells still dominated despite rapid persister formation. After 1 h of ampicillin treatment, the surviving cells comprised 48% susceptible cells, 28% pre-existing persisters, and 24% drug-induced persisters. In contrast, ciprofloxacin or kanamycin eliminated nearly all susceptible cells within 1 h, yielding survivors composed of 52% pre-existing and 47% induced persisters for ciprofloxacin, and 51% pre-existing and 49% induced persisters for kanamycin. Notably, the apparent balance between pre-existing and drug-induced persisters depends strongly on the seed dilution in SDTK assays; at high dilutions (e.g., 10,000-fold), survivors are dominated by induced persisters (Fig. S3b,c).

Drug-specific differences reveal nested relationships among persister subsets along a spectrum of persistence

Across all three antibiotics, we consistently observed the emergence of small colonies in agar plates beginning with samples taken at ~30 minutes of drug exposure, especially under ciprofloxacin and kanamycin treatment (Fig. 5d). These colonies typically became visible after an additional incubation for 2-3 days at room temperature following 20-h incubation at 37°C. Prolonged lag times and reduced

growth are hallmarks of stressed, metabolically impaired, or partially damaged cells—phenotypes frequently observed during recovery from stationary phase, starvation, or other stressors [14,39–41]. These observations illustrate that persister cells are highly heterogeneous. Upon antibiotic exposure, some cells encounter more severe damage than others and thus require longer recovery time before forming visible colonies on LB agar, resulting in variable colony sizes. This variability does not result from genetic mutations: when regrown, these persister cells formed normal-sized colonies indistinguishable from untreated wild type (Fig. S5).

Orders of magnitude difference in pre-existing persister fractions across antibiotics (Fig. 3d, 5a) suggest that cells persistent to one antibiotic are not necessarily persistent to another. These distinct fractions of pre-existing persisters also indicate substantial heterogeneity within the persister pool and drug-dependent thresholds for survival. Consistent with this interpretation, when multiple antibiotics were applied to the same exponential-phase culture, the resulting time-kill curves failed to extrapolate to a shared initial point (Fig. S4a vs. Fig. S4b and Fig. 6a). The different apparent “initial” persister frequency for each antibiotic supports a model in which different antibiotics induce and reveal specific persister subsets distributed along a continuum of tolerance.

To resolve the relationship between different persister subpopulations selected and induced by distinct antibiotics, we developed sequential-drug treatment experiments. Exponential phase cultures were first exposed to one antibiotic for 2 hours, after which surviving persisters were washed, split, and challenged with either a second drug or the same drug again as a control. The experiments were then repeated with a reverse treatment order for the two antibiotics. This design enables us to determine whether persisters to one drug exhibit cross-persistence against another drug, thereby revealing the relative strength of drug-specific persistence.

Importantly, this approach also allows us to identify nested hierarchical relationships among persister subpopulations. Persister subsets selected and induced by two antibiotics can exhibit three possible relationships: (i) two non-overlapping subsets, (ii) partially overlapping subsets, or (iii) one subset fully embedded within the other (Fig. 6b), as proposed previously [31]. Each relationship generates distinct predictions for sequential-drug treatments. When persister subsets are non-overlapping (relationship (i)), switching drugs results in rapid mutual elimination because each persister subset falls within the susceptible range of the other antibiotic. If two subsets partially overlap (relationship (ii)), each antibiotic should quickly eliminate the non-overlapping fraction of the other’s persisters. In contrast, when one drug’s persister subset is embedded within another (relationship (iii)), treatment with the former antibiotic should rapidly reduce the larger persister subset to a size comparable to the smaller, more persistent subset, whereas treatment with the latter should have little effect on the former’s persisters over a several-hour time window. Thus, sequential-drug treatments provide a direct means to resolve the hierarchical organization of persister subsets and their relative position along the persistence spectrum.

Sequential-drug treatments revealed a clear nested hierarchical relationship between the subsets of ampicillin and kanamycin persisters. Ampicillin persisters, which declined slowly under continued ampicillin exposure, were rapidly eliminated upon subsequent kanamycin treatment, producing biphasic killing dynamics (Fig. 6c) nearly identical to kanamycin-only controls (Fig. 2a, Fig. 6a,d). This ~3-log reduction demonstrates that most ampicillin persisters are not tolerant to kanamycin. In contrast, reversing the treatment order showed that ampicillin had minimal impact on kanamycin persisters, whose survival closely resembled PBS controls (Fig. 6d). The modest decline observed under ampicillin or PBS likely reflects post-stress death driven by delayed metabolic toxicity rather than direct ampicillin-mediated killing [42]. Together, these results indicate that kanamycin persisters are cross-tolerant to ampicillin but not vice versa, establishing kanamycin persisters as a more persistent subpopulation.

Consistent with the embedded relationship between persister subsets (Fig. 6b), kanamycin persisters constitute a highly refractory population nested within the broader ampicillin-persister pool (Fig. 6e). Prolonged antibiotic exposure progressively enriched for increasingly tolerant cells, revealing additional slower-killing phases after extended treatment (24 h; Fig. S6). Persisters surviving long-term ampicillin exposure exhibited substantially reduced clearance upon kanamycin challenge compared with those surviving shorter ampicillin exposure (~1-log versus ~3-log reduction; Fig. S7a vs. Fig. 6c), indicating enrichment of a highly persistent subset corresponding to kanamycin persisters. The long-tail behavior has similarly been reported for lag times, recovery dynamics, and long-term killing kinetics [43,44], indicating heterogeneity along the persistence continuum. These and our observations support a nested structure in which extended antibiotic exposure selectively enriches for increasingly tolerant states along a persistence spectrum.

Further sequential-drug treatment experiments resolved the nested relationships among ampicillin, ciprofloxacin, and kanamycin persisters. Most ampicillin persisters were rapidly eliminated by ciprofloxacin, yielding biphasic killing dynamics (Fig. 6f), whereas prolonged ampicillin exposure enriched for a ciprofloxacin-tolerant subset (Fig. S7b). Conversely, ciprofloxacin persisters were largely unaffected by subsequent ampicillin treatment (Fig. 6g), indicating higher persistence. Finally, ciprofloxacin persisters were rapidly eliminated by kanamycin, while kanamycin persisters remained tolerant to ciprofloxacin (Fig. 6i,j). Sequential-drug treatments of cultures grown from 100-fold dilution (~90% pre-existing persisters, Fig. 2d) and from 1,000-fold dilution (~50% induced persisters, Fig. 2d) revealed the same patterns: ampicillin persisters were rapidly killed by sequential ciprofloxacin or kanamycin treatment but not vice versa (Fig. S8 vs. Fig. 6f,g,i). The findings confirm that pre-existing and drug-induced persisters share the same nested hierarchical relationships and both exhibit heterogeneous tolerance spanning across a spectrum.

Together, these results establish a nested persistence hierarchy in which kanamycin persisters represent the most tolerant subset, embedded within ciprofloxacin persisters, which are themselves a subset of ampicillin persisters (Fig. 6k). This framework supports a continuum model of persistence, explaining drug-specific cross-tolerance patterns and revealing how different antibiotics induce and select nested regions across the persistence spectrum.

Discussion

In this study, we establish a quantitative framework by integrating kinetic modeling with a new strategy: serial-dilution time–kill (SDTK) assays. This approach enables accurate quantification of both pre-existing and drug-induced persisters within the same population—subpopulations that are otherwise operationally indistinguishable. Importantly, the SDTK framework resolves the challenge of measuring a biological variable (e.g., persister abundance) that is itself perturbed by the measurement process (e.g., time–kill assays). Using this strategy, we validate the drug-induced persister model and resolve population-level persister dynamics during antibiotic treatment without relying on specialized single-cell techniques. By circumventing key limitations of single-cell approaches, including low throughput, limited resolution, and dependence on reliable molecular markers, this framework enables quantitative analysis of extremely rare persister subpopulations.

Although the integrated SDTK approach allows simultaneous quantification of subpopulations, the accuracy of determining pre-existing persisters (P_0) could be compromised when pre-existing persister fractions are extremely low. When cultures are extremely diluted, drug-induced persisters dominate (e.g., >99%), making the fractions of pre-existing persisters negligible and thus insensitive to model fitting. In practice, moderately diluted cultures provide the most reliable estimates. A simpler, coarse-grained alternative to SDTK quantification of persisters is to extrapolate the slow killing phase to time zero using minimally diluted cultures (e.g., ≤100-fold dilution, in which drug-induced persister fractions varied by <15%) (Fig. 2d). This simplified approach provides better estimates of persister cells than the conventional single time-point CFU counts but should be considered an upper-bound estimate of pre-existing persister subpopulation size.

Our drug-induced kinetic model focuses on the first 7-8 hours of antibiotic exposure, during which biphasic killing predominates, but additional killing phases can emerge with prolonged treatment [8]. Indeed, extending exposure to 24 hours reveals a multi-phase pattern consisting of rapid killing of susceptible cells, slower decay of most persisters, and an even slower phase corresponding to ultra-persistent cells (Fig. S6). These highly refractory cells represent fewer than 10^{-8} of the initial population and are several orders of magnitude rarer than the predominant persisters captured by our model. Therefore, excluding these ultra-rare subpopulations does not affect our model's accuracy. The biphasic framework provides a robust and reliable description of drug-induced persister dynamics over our experimental timescale.

Differences in persister frequencies and killing dynamics across antibiotics can be largely explained by their distinct modes of action and metabolic dependencies. Ampicillin, a β-lactam whose activity strongly depends on metabolism, is ineffective against slow-growing or dormant cells [45]. Growth arrest under acute ampicillin stress is sufficient to convert cells into persisters, producing the largest pre-existing persister fraction and the rapidest induction of new persisters (Figs. 2,3). Ciprofloxacin, in contrast, remains effective against non-growing cells through lethal DNA damage [45], resulting in smaller pre-existing persister fractions. Survival requires activation of additional stress-response pathways, such

as SOS-mediated DNA repair, yielding a smaller but more refractory persister subset. Kanamycin, an aminoglycoside, irreversibly disrupts ribosomes [46], cell membranes and the cytoplasm [47,48]. With the least metabolic dependence among the three antibiotics tested [45], kanamycin rapidly eliminates susceptible cells and most Amp and Cip persisters (Fig. 6), leaving the rarest but most tolerant survivors. These differences together with differential cellular responses to antibiotics [49] explain why ampicillin, ciprofloxacin, and kanamycin select and generate distinct persistence phenotypes.

Interestingly, despite being less potent than ciprofloxacin against susceptible cells, ampicillin kills persisters faster (greater k_2) than ciprofloxacin (Fig. 3b,c). This apparent paradox likely reflects differences in the persister states generated: ampicillin readily selects and produces new persisters, but these cells are under a less protected physiological state and are therefore more easily killed, whereas ciprofloxacin generates fewer persisters, but they are considerably more recalcitrant. Differences in target accessibility and binding reversibility may further contribute: ampicillin irreversibly inhibits penicillin-binding proteins on cell surfaces [50], whereas ciprofloxacin must enter the cell before binding to DNA-associated enzymes, resulting in relatively weak and reversible drug-enzyme-DNA complexes when the drug is removed [51,52].

Our results demonstrate that persistence is heterogeneous and spans across a spectrum of tolerance. Sequential-drug treatments and extended time-kill analyses reveal nested hierarchies of persister subpopulations (Fig. 6k). Prolonged exposure progressively enriches for increasingly persistent cells with slower killing kinetics (Fig. S6 and S7). This graded heterogeneity is supported by single-cell observations that persisters vary widely in growth rate, lag time, ribosome content, metabolic activity, and stress responses [22–24,43,53–55]. The slow-growing colonies of different sizes observed after prolonged incubation in our assays and others [14,39] likely reflect these graded states and recovery capacities. Even persisters with the same persistence can arise from various combinations of target inactivation, cellular damage, and stress-triggered defense and repair programs. Despite the substantial heterogeneity among persisters, there is no evidence showing that pre-existing persisters differ from drug-induced persisters.

Here, we propose a Drug-Induced Persistence Spectrum (DIPS) model describing the formation and dynamics of heterogeneous persisters during antibiotic treatment (Fig. 7). Antibiotic persisters are not created equal. At the onset, the stationary-phase inoculum exhibits a wide range of dormancy depths and lag times [43,55]. Upon transfer to fresh medium, most cells rapidly resume growth, whereas a small heterogeneous fraction remains dormant, metabolically slow, or in an adaptive state, constituting the pre-existing persister pool. Once exposed to antibiotics, exponentially growing cells undergo acute stress and extensive injury, and the majority are rapidly eliminated with a high killing rate constant (k_1) before protective pathways can be activated. A minority, however, successfully activate sufficient stress-induced responses to repair DNA, protein, and/or membrane damage, surviving the primary attack and drug-induced reactive species [42,56–58]. These cells thus transition into persisters at a drug-specific formation rate (f_1), acquiring various degrees of persistence strength. When drug-inflicted damages

exceed the capacity of defense and repair systems, both pre-existing and drug-induced persisters are ultimately eliminated with a slower killing rate constant (k_2).

Ampicillin selects and generates the largest but weakest persister subset, ciprofloxacin induces an intermediate subset, and kanamycin yields a rare, highly refractory subset. These subsets form a nested hierarchy across the persistence spectrum, with kanamycin persisters embedded within ciprofloxacin persisters, which are themselves nested within the broader ampicillin-persister pool (Fig 7). The spectrum of persistence yields sequential long-term killing dynamics: rapid elimination of susceptible cells followed by progressively slower decay of increasingly tolerant persisters. The resulting long-tailed kinetics can be described by a power-law or Weibull model [43,44,59], while short-term dynamics are well approximated by biphasic exponential decay.

This DIPS framework reconciles divergent observations in persister profiles across antibiotics [10,31,60]. More broadly, it can be generalized into a “stress-induced-persistence-spectrum” model, as environmental stresses such as heat, low pH, oxidative stress, hazardous chemicals, bacteriostatic agents, and starvation also trigger antibiotic persistence [7,8,61,62]. These stresses cause varying degrees of cellular damage and induce different levels of defense and repair mechanisms in bacterial cells, resulting in heterogeneity in persistence. Because antibiotics differ in their propensity to induce and enrich tolerant subpopulations, treatment can select highly persistent cells even without genetic resistance. Incorporating drug-induced persistence profiles alongside MIC evaluations may therefore guide antibiotic choice and improve strategies to limit persister emergence and accelerate clearance.

Conclusion

This study establishes a quantitative framework that resolves the longstanding challenge of distinguishing drug-induced persisters from pre-existing persisters. By integrating SDTK assays with kinetic modeling, we reveal their population dynamics during antibiotic treatment. We show that antibiotics differ not only in killing potency but also in their capacity to induce persister formation, generating heterogeneous subpopulations that span a continuum of tolerance. The framework further enables identification of genetic determinants that specifically regulate pre-existing persistence and/or persister formation during treatment. Through systematic sequential-drug treatments, we uncover nested hierarchical relationships among antibiotic-specific persister subsets. Together, we propose a Drug-Induced Persister Spectrum (DIPS) model in which antibiotics both induce and select subsets with distinct tolerance. Beyond bacterial systems, our framework provides a generalizable strategy for dissecting treatment-induced persistence in fungal pathogens and cancer cells implicated in therapeutic failure and relapse.

Methods and Materials

Model development

In time-kill assays, antibiotic persistence can be characterized by biphasic killing kinetics, with a rapid elimination phase of susceptible cells followed by a slow killing phase of persisters. In these assays, stationary-phase cultures are diluted into pre-warmed fresh medium and grown to the exponential phase before antibiotic addition. At the time of drug exposure, the population is assumed to consist of two major subpopulations: susceptible cells (*S*) and persister cells (*P*). Spontaneously formed persisters arising during exponential growth are presumed to be negligible compared with the pre-existing persisters inherited from the stationary phase. Thus, although more heavily diluted cultures require longer times to reach the same density, the number of spontaneous persisters in all dilutions is assumed to remain negligible (discussed in the main text). Thus, spontaneous persister formation is omitted in our drug-induced persister model.

Pre-existing persisters are defined as the fraction of cells in the persister state at the onset of antibiotic exposure. Accordingly, the persister fraction carried over from the stationary-phase inoculum is assumed not to expand during cultivation, despite potentially retaining low metabolic activity of the persisters [29]. Although single-cell studies have reported that a small fraction of persisters can grow and even propagate prior to antibiotic exposure [22,23,63], this behavior does not affect the validity and accuracy of our model or the interpretation of the SDTK experiments. Any potential propagation of pre-existing persisters would occur proportionally across serially diluted cultures and therefore preserve dilution scaling predicted by a pre-existing-only model (Fig. 1b). Moreover, although persister growth is possible [14,23,24,63,64], propagation, if it occurs at all, appears restricted to a minority of persister cells and does not substantially increase the pre-existing persister number. The effect of persister propagation would therefore be minimal compared with the total number of pre-existing and drug-induced persisters. Thus, the drug-induced persister model remains robust, even without explicitly incorporating the rare persister multiplication.

Both *P* and *S* subpopulations are killed independently, with rate constants k_1 for susceptible cells and k_2 for persisters. The population dynamics during antibiotic exposure are therefore described as:

$$\frac{dS}{dt} = \mu * S - k_1 * S - f_1 * S \quad (1)$$

$$\frac{dP}{dt} = f_1 * S - k_2 * P \quad (2)$$

$$N = P + S \quad (3)$$

Here, f_1 represents the rate constant of drug-induced persister formation. The classical pre-existing-persister model is a special case of this framework, in which $f_1 = 0$, and no additional persisters form during treatment. All parameters and variables, including f_1, k_1, k_2, S_0 (initial susceptible population), and

P_0 (initial persister population), were obtained from experimental measurements and model fitting. We assume that bacterial growth halts immediately upon drug supplement ($\mu = 0$).

Strains and growth conditions

The wild-type *E. coli* strain MG1655 was used for most experiments. Two knockout strains, including *Δppk* and *ΔrelAΔspoT*, each derived from MG1655, were kindly provided by Gray lab [33,65] and used to assess the roles of polyphosphate kinase (PPK) and the ppGpp in persister formation. Cultures were grown in Luria–Bertani (LB; Miller formulation) medium with or without antibiotics. Three bactericidal antibiotics with distinct modes of action were examined: ampicillin (Amp) targeting cell wall synthesis; ciprofloxacin (Cip) targeting DNA gyrase; and kanamycin (Kan) targeting the ribosome. Drug stocks were freshly prepared and stored at −20 °C. Amp solutions were stored at −80 °C and used within two months. Unless otherwise noted, antibiotics were applied at 10× MIC. For turbidostatic experiments, a continuous-culture device (Chi.Bio) [66] was used to maintain exponential-phase growth (OD_{600} ≈ 0.6) for ~12 h prior to initiating SDTK assays.

Serial-dilution time-kill (SDTK) assays

Single colonies were grown overnight in LB, diluted 1:100,000 into fresh LB medium, and cultured for 18 h to generate seed cultures. We used this two-step cultivation to minimize experimental variations and the potential age effect on antibiotic persistence [67]. These were then serially diluted 100×, 1,000×, or 10,000× into pre-warmed fresh LB medium. Cultures were grown to early exponential phase with OD_{600} ≈ 0.6 (~2–3 × 10^8 cells ml^{-1}) before antibiotic addition. Samples were collected at defined intervals for 6–8 h. After sampling, antibiotics were removed by washing, and cells were plated on antibiotic-free LB agar plates. Plates were incubated at 37 °C for 20 h and then held at room temperature for an additional 2 days to allow small colonies to emerge. For kanamycin-treated samples where killing was substantially faster, cultures were concentrated prior to plating, and plates were kept at room temperature for another three days for small colonies to appear before CFU enumeration.

MIC determination

Minimum inhibitory concentrations (MICs) were measured for the wild type, *ΔrelAΔspoT*, and *ΔppK* strains following previously described protocols [68] with slight modification. Each of the three antibiotics (ampicillin, ciprofloxacin, and kanamycin) was serially diluted 2-fold in LB medium in 96-well microtiter plates. Overnight cultures were then diluted into fresh LB medium and grown to the exponential phase (~ 2-3 h), then further diluted in pre-warmed LB medium and inoculated into the wells containing the antibiotic dilutions at the same initial cell density (OD_{600}= ~0.02). After incubation at 37 °C overnight, OD_{600} values were measured using a plate reader (Molecular Devices, Inc.) to assess bacterial growth. Fresh medium without inoculum was used as blank controls. The MIC for each drug-strain combination was defined as the lowest antibiotic concentration at which no increase in OD_{600} was observed.

Sequential antibiotic treatments

Seed cultures prepared as described above were diluted into fresh medium and grown to an OD_{600} of 0.6 before the addition of a primary antibiotic. Unless otherwise mentioned, two hours after exposure, the drug was removed by centrifuging the cultures at 37 °C and resuspending the pellets in pre-warmed LB medium supplemented either with a second antibiotic (for sequential treatment) or with the same antibiotic (for continuous single-drug treatment). The cultures were then centrifuged and resuspended once more in the same pre-warmed LB medium to ensure complete removal of the primary drug. As a control, after removal of the primary antibiotic, cultures were washed and resuspended in pre-warmed phosphate-buffered saline (PBS). Samples were collected at defined time intervals, and surviving cells were enumerated by CFU plating.

Extended-exposure experiments were performed as described above, except that the duration of the initial antibiotic treatment was prolonged as indicated in the Results. Unless otherwise noted, cultures derived from 100-fold diluted inocula were used to ensure that mainly pre-existing persisters were analyzed while minimizing the confounding effect of drug-induced persisters. To assess both pre-existing and drug-induced persister subsets, cultures derived from 1,000-fold diluted inocula were treated using the same protocol.

Model fitting

Kinetic models were simulated and fitted to experimental SDTK data using MATLAB (version 2024b, MathWorks Inc.). Model dynamics were simulated using the "ode45()" solver. For fitting, parameters k_1 and k_2 were fitted to the first and second linear regions, respectively, of the log-transformed viable cell counts using the first-order (linear) polyfit() function. Then, lsqnonlin() performed simultaneous fitting of P_0 for the least diluted culture (e.g., 100×) and f_1 for all cultures. P_0 values for the more dilute cultures were set by the corresponding dilution factors. For turbidostat-Amp fits, the initial persister percent, P_0 %, was assumed to be 8×10^{-5} based on simulations (Fig S2d, Table S1) of a previously published spontaneous persister formation model [14].

The same linear regression approach was used to fit sequential-treatment data exhibiting monophasic or biphasic killing kinetics. For better visualization of these data, drug-induced persister formation was not explicitly modeled because the formation rate (f_1) cannot be estimated without serial dilution and was thus set to zero. This simplification does not affect the identification of the nested hierarchy among persister subsets.

Statistical methods

All statistical analyses were performed using GraphPad Prism (Version 10.2.3). Group differences were assessed by one-way ANOVA, followed by Tukey's Honest Significant Difference (HSD) post hoc test, with significance set at $\alpha < 0.05$. When assumptions of normality were violated, the nonparametric

Kruskal–Wallis test was applied. When normality was met but variances were unequal, Brown–Forsythe or Welch ANOVA was used, followed by Dunnett's post hoc test for multiple comparisons.

Declarations

Data availability

All data used in this study are available in the main manuscript and the Supplementary material files; raw data are available upon request.

Code availability

All code files and related data used in this study are available in the GitHub repository: https://github.com/schultz-lab/persisters.

Acknowledgements

We thank Dr. Michal Gray at the University of Alabama at Birmingham for kindly providing the *E coli MG1655 Δppk* and *ΔrelAΔspoT* strains. We thank Wolfgang L. Weber, Iam A. Cucho, and Eunice A. Antwi for their assistance in collecting experimental data.

Funding

This research was supported in part by National Science Foundation (NSF) CCF Division grant 2240264 and funding from Dartmouth College, awarded to Rahul Sarpeshkar. This work was also supported in part by NSF grants PHY-2412766 and DMS-2527337 as well as the U.S. Department of Energy grant DE-SC0026232, awarded to Daniel Schultz.

Competing interests

The authors declare no competing interests.

Contributions

Y.D. and R.S. conceived the project. **Y.D.** designed the experiments with inputs from **D.R.B** and **D.S**. **Y.D. and D.R.B.** developed the models. **Y.D., H.E.M., and K.K.E.** performed the experiments and collected the data. **D.R.B.** performed model simulations and data fitting. **D.R.B. and Y.D.** analyzed the data and prepared the figures. **R.S. and D.S.** secured the funding and resources. **Y.D.** wrote the manuscript. **Y.D., D.R.B., D.S., and R.S.** revised the manuscript. All authors reviewed and approved the final manuscript.

References

1. Murray, C. J. *et al.* Global burden of bacterial antimicrobial resistance in 2019: a systematic analysis. *Lancet* **399**, 629–655 (2022).

2. Fisher, R. A., Gollan, B. & Helaine, S. Persistent bacterial infections and persister cells. *Nat. Rev. Microbiol.* **15**, 453–464 (2017).
3. Bakkeren, E., Diard, M. & Hardt, W.-D. Evolutionary causes and consequences of bacterial antibiotic persistence. *Nat. Rev. Microbiol.* **18**, 479–490 (2020).
4. Lewis, K. Persister Cells. *Annu. Rev. Microbiol.* **64**, 357–372 (2010).
5. Windels, E. M. *et al.* Bacterial persistence promotes the evolution of antibiotic resistance by increasing survival and mutation rates. *ISME J.* **13**, 1239–1251 (2019).
6. Bigger, J. Treatment of staphylococcal infections with penicillin by intermittent sterilization. *Lancet* **244**, 497–500 (1944).
7. Keren, I., Kaldalu, N., Spoering, A., Wang, Y. & Lewis, K. Persister cells and tolerance to antimicrobials. *FEMS Microbiol. Lett.* **230**, 13–18 (2004).
8. Balaban, N. Q. *et al.* Definitions and guidelines for research on antibiotic persistence. *Nat. Rev. Microbiol.* **17**, 441–448 (2019).
9. Song, S. & Wood, T. K. ppGpp ribosome dimerization model for bacterial persister formation and resuscitation. *Biochem. Biophys. Res. Commun.* **523**, 281–286 (2020).
10. Harms, A., Maisonneuve, E. & Gerdes, K. Mechanisms of bacterial persistence during stress and antibiotic exposure. *Science* **354**, (2016).
11. Zhang, Y. Persisters, persistent infections and the Yin–Yang model. *Emerg. Microbes Infect.* **3**, 1–10 (2014).
12. Podlesek, Z. & Žgur Bertok, D. The DNA Damage Inducible SOS Response Is a Key Player in the Generation of Bacterial Persister Cells and Population Wide Tolerance. *Front. Microbiol.* **11**, (2020).
13. Niu, H., Gu, J. & Zhang, Y. Bacterial persisters: molecular mechanisms and therapeutic development. *Signal Transduct. Target. Ther.* **9**, 174 (2024).
14. Balaban, N. Q., Merrin, J., Chait, R., Kowalik, L. & Leibler, S. Bacterial persistence as a phenotypic switch. *Science* **305**, 1622–1625 (2004).
15. Manuse, S. *et al.* Bacterial persisters are a stochastically formed subpopulation of low-energy cells. *PLoS Biol.* **19**, (2021).
16. Rotem, E. *et al.* Regulation of phenotypic variability by a threshold-based mechanism underlies bacterial persistence. *Proc. Natl. Acad. Sci.* **107**, 12541–12546 (2010).
17. Levin, B. R., Concepción-Acevedo, J. & Udekwu, K. I. Persistence: a copacetic and parsimonious hypothesis for the existence of non-inherited resistance to antibiotics. *Curr. Opin. Microbiol.* **21**, 18–21 (2014).
18. Johnson, P. J. T. & Levin, B. R. Pharmacodynamics, Population Dynamics, and the Evolution of Persistence in Staphylococcus aureus. *PLoS Genet.* **9**, e1003123 (2013).
19. Dörr, T., Lewis, K. & Vulić, M. SOS Response Induces Persistence to Fluoroquinolones in Escherichia coli. *PLoS Genet.* **5**, e1000760 (2009).

20. Dörr, T., Vulić, M. & Lewis, K. Ciprofloxacin Causes Persister Formation by Inducing the TisB toxin in Escherichia coli. *PLoS Biol.* **8**, e1000317 (2010).
21. Greve, N. B., Slotved, H.-C., Olsen, J. E. & Thomsen, L. E. Identification of antibiotic induced persister cells in Streptococcus agalactiae. *PLoS One* **19**, e0303271 (2024).
22. Orman, M. A. & Brynildsen, M. P. Dormancy Is Not Necessary or Sufficient for Bacterial Persistence. *Antimicrob. Agents Chemother.* **57**, 3230–3239 (2013).
23. Goormaghtigh, F. & Van Melderen, L. Single-cell imaging and characterization of Escherichia coli persister cells to ofloxacin in exponential cultures. *Sci. Adv.* **5**, (2019).
24. Kim, J., Yamasaki, R., Song, S., Zhang, W. & Wood, T. K. Single cell observations show persister cells wake based on ribosome content. *Environ. Microbiol.* **20**, 2085–2098 (2018).
25. El Meouche, I., Jain, P., Jolly, M. K. & Capp, J.-P. Drug tolerance and persistence in bacteria, fungi and cancer cells: Role of non-genetic heterogeneity. *Transl. Oncol.* **49**, 102069 (2024).
26. Russo, M. *et al.* Cancer drug-tolerant persister cells: from biological questions to clinical opportunities. *Nat. Rev. Cancer* **24**, 694–717 (2024).
27. Sharma, S. V. *et al.* A Chromatin-Mediated Reversible Drug-Tolerant State in Cancer Cell Subpopulations. *Cell* **141**, 69–80 (2010).
28. Rosenberg, A. *et al.* Antifungal tolerance is a subpopulation effect distinct from resistance and is associated with persistent candidemia. *Nat. Commun.* **9**, 2470 (2018).
29. Rahman, K. M. T. *et al.* Rethinking dormancy: Antibiotic persisters are metabolically active, non-growing cells. *Int. J. Antimicrob. Agents* **65**, 107386 (2025).
30. Manina, G. & McKinney, J. D. A Single-Cell Perspective on Non-Growing but Metabolically Active (NGMA) Bacteria. in *Pathogenesis of Mycobacterium tuberculosis and its Interaction with the Host Organism* 135–161 (2013). doi:10.1007/82_2013_333.
31. Shultis, M. W., Mulholland, C. V. & Berney, M. Are all antibiotic persisters created equal? *Front. Cell. Infect. Microbiol.* **12**, (2022).
32. Gray, M. J. & Jakob, U. Oxidative stress protection by polyphosphate—new roles for an old player. *Curr. Opin. Microbiol.* **24**, 1–6 (2015).
33. Hamm, C. W. & Gray, M. J. Inorganic polyphosphate and the stringent response coordinately control cell division and cell morphology in Escherichia coli. *MBio* **16**, (2025).
34. Chowdhury, N., Kwan, B. W. & Wood, T. K. Persistence Increases in the Absence of the Alarmone Guanosine Tetraphosphate by Reducing Cell Growth. *Sci. Rep.* **6**, 20519 (2016).
35. Korch, S. B., Henderson, T. A. & Hill, T. M. Characterization of the hipA7 allele of Escherichia coli and evidence that high persistence is governed by (p)ppGpp synthesis. *Mol. Microbiol.* **50**, 1199–1213 (2003).
36. Fritsch, V. N. *et al.* The alarmone (p)ppGpp confers tolerance to oxidative stress during the stationary phase by maintenance of redox and iron homeostasis in Staphylococcus aureus. *Free Radic. Biol. Med.* **161**, 351–364 (2020).

37. Qi, W., Jonker, M. J., de Leeuw, W., Brul, S. & ter Kuile, B. H. Role of RelA-synthesized (p)ppGpp and ROS-induced mutagenesis in de novo acquisition of antibiotic resistance in E. coli. *iScience* **27**, 109579 (2024).
38. Bergum, O. E. T. *et al.* SOS genes are rapidly induced while translesion synthesis polymerase activity is temporally regulated. *Front. Microbiol.* **15**, (2024).
39. Vulin, C., Leimer, N., Huemer, M., Ackermann, M. & Zinkernagel, A. S. Prolonged bacterial lag time results in small colony variants that represent a sub-population of persisters. *Nat. Commun.* **9**, (2018).
40. Guillier, L., Pardon, P. & Augustin, J.-C. Influence of Stress on Individual Lag Time Distributions of Listeria monocytogenes. *Appl. Environ. Microbiol.* **71**, 2940–2948 (2005).
41. Levin-Reisman, I. *et al.* Automated imaging with ScanLag reveals previously undetectable bacterial growth phenotypes. *Nat. Methods* **7**, 737–739 (2010).
42. Hong, Y., Zeng, J., Wang, X., Drlica, K. & Zhao, X. Post-stress bacterial cell death mediated by reactive oxygen species. *Proc. Natl. Acad. Sci.* **116**, 10064–10071 (2019).
43. Şimşek, E. & Kim, M. Power-law tail in lag time distribution underlies bacterial persistence. *Proc. Natl. Acad. Sci.* **116**, 17635–17640 (2019).
44. Rebelo, J. S., Domingues, C. P. F., Monteiro, F., Nogueira, T. & Dionisio, F. Bacterial persistence is essential for susceptible cell survival in indirect resistance, mainly for lower cell densities. *PLoS One* **16**, e0246500 (2021).
45. Zheng, E. J., Stokes, J. M. & Collins, J. J. Eradicating Bacterial Persisters with Combinations of Strongly and Weakly Metabolism-Dependent Antibiotics. *Cell Chem. Biol.* **27**, 1544-1552.e3 (2020).
46. Davis, B. D. Mechanism of bactericidal action of aminoglycosides. *Microbiological Reviews* vol. 51 341–350 (1987).
47. Wohlgemuth, I. *et al.* Translation error clusters induced by aminoglycoside antibiotics. *Nat. Commun.* **12**, 1830 (2021).
48. Wong, F. *et al.* Cytoplasmic condensation induced by membrane damage is associated with antibiotic lethality. *Nat. Commun.* **12**, (2021).
49. Mattiello, S. P., Barth, V. C., Scaria, J., Ferreira, C. A. S. & Oliveira, S. D. Fluoroquinolone and beta-lactam antimicrobials induce different transcriptome profiles in Salmonella enterica persister cells. *Sci. Rep.* **13**, 18696 (2023).
50. Beadle, B. M., Nicholas, R. A. & Shoichet, B. K. Interaction energies between β-lactam antibiotics and E. coli penicillin-binding protein 5 by reversible thermal denaturation. *Protein Sci.* **10**, 1254–1259 (2001).
51. Maglica, Ž., Özdemir, E. & McKinney, J. D. Single-cell tracking reveals antibiotic-induced changes in mycobacterial energy metabolism. *MBio* **6**, e02236-14 (2015).
52. Mustaev, A. *et al.* Fluoroquinolone-gyrase-DNA complexes: two modes of drug binding. *J. Biol. Chem.* **289**, 12300–12 (2014).

53. Ma, P. *et al.* Bacterial droplet-based single-cell RNA-seq reveals antibiotic-associated heterogeneous cellular states. *Cell* **186**, 877-891.e14 (2023).
54. Stevanovic, M., Teuber Carvalho, J. P., Bittihn, P. & Schultz, D. Dynamical model of antibiotic responses linking expression of resistance genes to metabolism explains emergence of heterogeneity during drug exposures. *Phys. Biol.* **21**, 036002 (2024).
55. Pu, Y. *et al.* ATP-Dependent Dynamic Protein Aggregation Regulates Bacterial Dormancy Depth Critical for Antibiotic Tolerance. *Mol. Cell* **73**, 143-156.e4 (2019).
56. Wong, F. *et al.* Reactive metabolic byproducts contribute to antibiotic lethality under anaerobic conditions. *Mol. Cell* **82**, 3499-3512.e10 (2022).
57. Kohanski, M. A., Dwyer, D. J., Hayete, B., Lawrence, C. A. & Collins, J. J. A Common Mechanism of Cellular Death Induced by Bactericidal Antibiotics. *Cell* **130**, 797–810 (2007).
58. Schultz, D., Palmer, A. C. & Kishony, R. Regulatory Dynamics Determine Cell Fate following Abrupt Antibiotic Exposure. *Cell Syst.* **5**, 509-517.e3 (2017).
59. Peleg, M. Modeling the dynamic kinetics of microbial disinfection with dissipating chemical agents —a theoretical investigation. *Appl. Microbiol. Biotechnol.* **105**, 539–549 (2021).
60. Brauner, A., Fridman, O., Gefen, O. & Balaban, N. Q. Distinguishing between resistance, tolerance and persistence to antibiotic treatment. *Nat. Rev. Microbiol.* **14**, 320–30 (2016).
61. Cotten, K. L. & Davis, K. M. Bacterial heterogeneity and antibiotic persistence: bacterial mechanisms utilized in the host environment. *Microbiol. Mol. Biol. Rev.* **87**, (2023).
62. Kwan, B. W., Valenta, J. A., Benedik, M. J. & Wood, T. K. Arrested protein synthesis increases persister-like cell formation. *Antimicrob. Agents Chemother.* **57**, 1468–1473 (2013).
63. Umetani, M. *et al.* Observation of persister cell histories reveals diverse modes of survival in antibiotic persistence. *Elife* **14**, (2025).
64. Kim, J.-S. *et al.* Bacterial persisters tolerate antibiotics by not producing hydroxyl radicals. *Biochem. Biophys. Res. Commun.* **413**, 105–110 (2011).
65. Gray, M. J. Inorganic Polyphosphate Accumulation in Escherichia coli Is Regulated by DksA but Not by (p) ppGpp. (2019).
66. Steel, H., Habgood, R., Kelly, C. L. & Papachristodoulou, A. In situ characterisation and manipulation of biological systems with Chi.Bio. *PLOS Biol.* **18**, e3000794 (2020).
67. Luidalepp, H., Jõers, A., Kaldalu, N. & Tenson, T. Age of inoculum strongly influences persister frequency and can mask effects of mutations implicated in altered persistence. *J. Bacteriol.* **193**, 3598–3605 (2011).
68. Barnes V, L., Heithoff, D. M., Mahan, S. P., House, J. K. & Mahan, M. J. Antimicrobial susceptibility testing to evaluate minimum inhibitory concentration values of clinically relevant antibiotics. *STAR Protoc.* **4**, 102512 (2023).

Figures

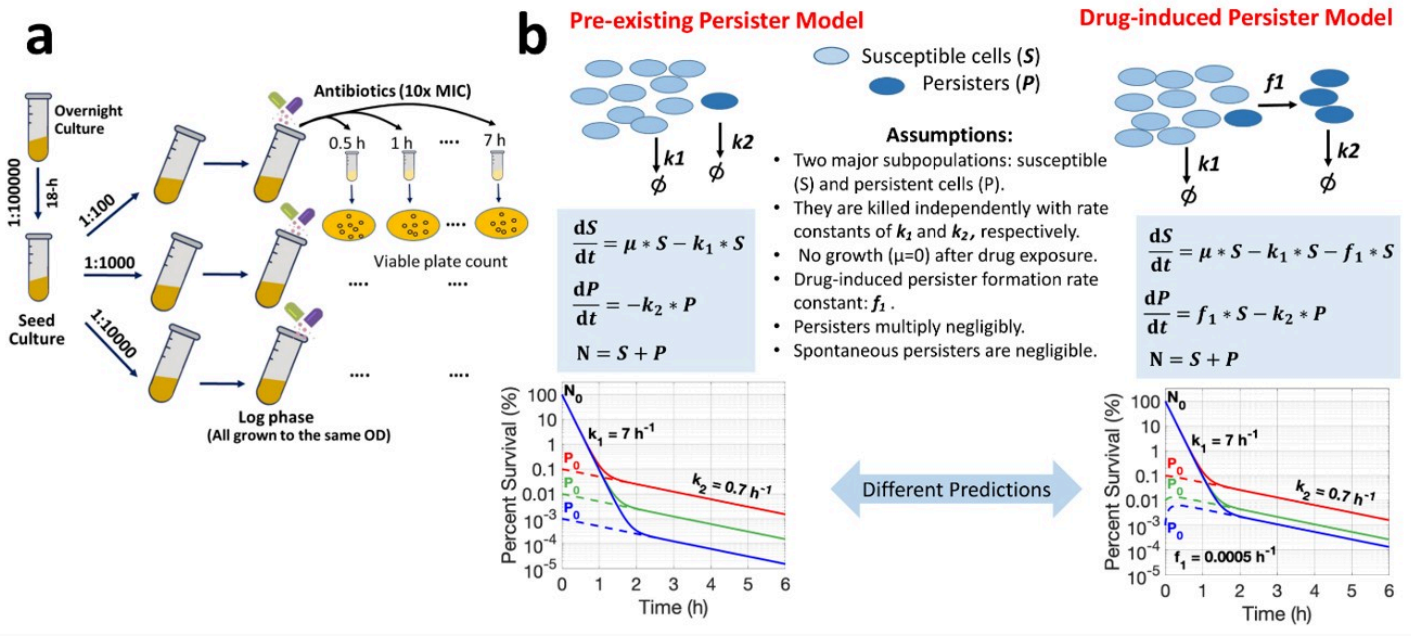


Figure 1

Methodology to distinguish two working models for antibiotic persistence. (a) Serial-dilution time-kill (SDTK) assay. Seed cultures are serially diluted in a fresh medium (e.g., 100x, 1,000x, 10,000x) and grown to an equal optical density at the exponential phase before exposure to antibiotics for standard time-kill assays. After drug removal, surviving cells are enumerated by counting colony-forming units (CFUs) using the viable plate count method. (b) Predictions of the pre-existing and drug-induced persister models. In the pre-existing model, all persisters exist prior to antibiotic exposure and are diluted proportionally with each serial dilution, resulting in evenly spaced secondary killing phases (10× serial dilution shown). In the drug-induced model, antibiotic stress induces additional persisters during treatment, causing the more diluted cultures—those with fewer pre-existing persisters—to show relatively elevated survival curves. Dashed curves denote the persister fraction, while solid curves denote the total population. Simulations were performed using biologically relevant parameters.

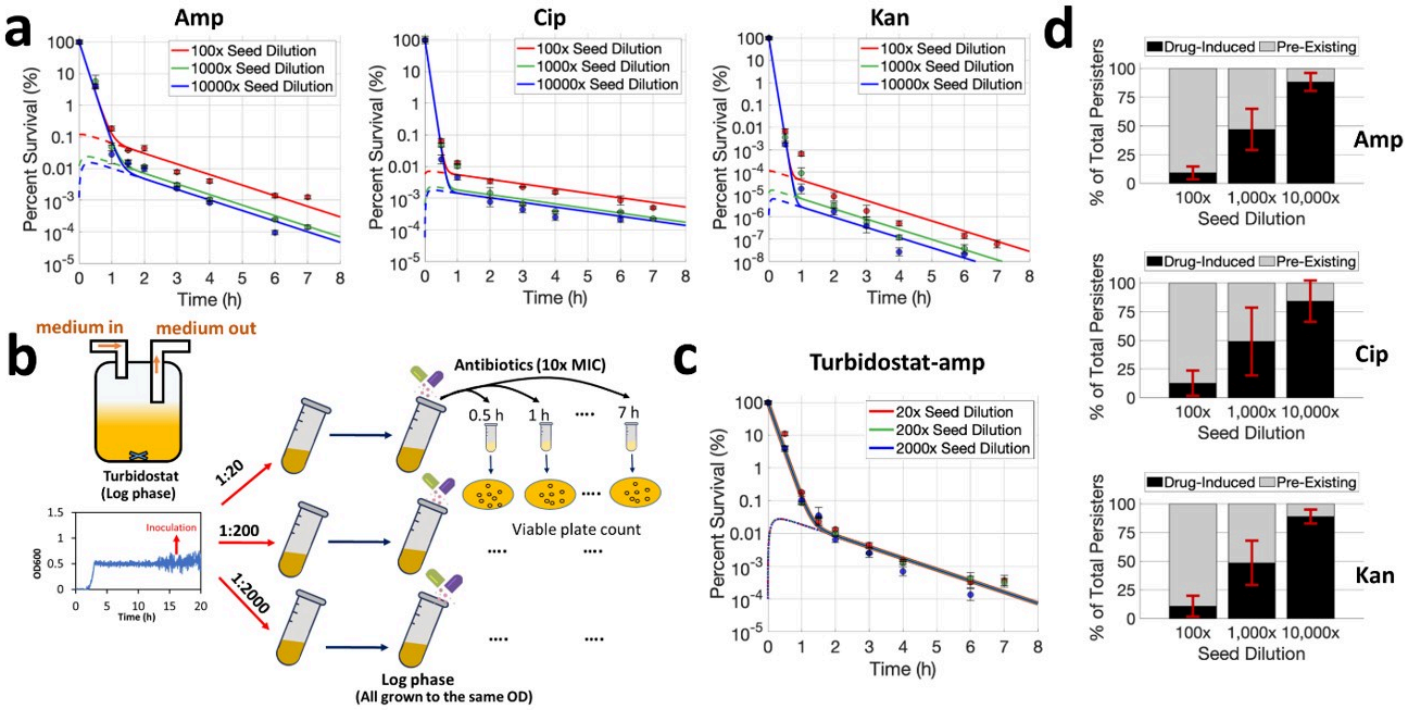


Figure 2

Experimental validation and quantification of drug-induced persister formation using SDTK assays. (A) SDTK assays of *E. coli* MG1655 treated with ampicillin (Amp, 80 μg/ml), ciprofloxacin (Cip, 1.25 μg/ml), or kanamycin (Kan, 320 μg/ml), each at 10× the minimal inhibitory concentration (MIC). Data were fitted using the drug-induced persister model. Shown are representative graphs from four replicates across two independent experiments. Dashed curves represent the persister subpopulation, whereas solid curves represent the total population. (b) Experimental setup for turbidostat-controlled growth followed by SDTK assays. Bacteria were maintained at constant optical density (OD_{600} = 0.6) during exponential growth for approximately 12 h in the turbidostat, effectively minimizing persisters carried over from the stationary-phase inoculum. After serial dilution into pre-warmed fresh medium, the resulting cultures were re-grown to the same OD_{600} values prior to ampicillin exposure. (c) SDTK assays of cultures derived from the turbidostatic experiments, with data fitted by the drug-induced persister model. (d) Relative fractions of drug-induced and pre-existing persisters within the total persister subpopulation for overnight batch experiments across different dilution factors. Fractions were calculated from data collected 3 h after antibiotic exposure, at which point the proportions had reached steady states. Data are presented as means ± standard deviation (SD) from at least three independent experiments.

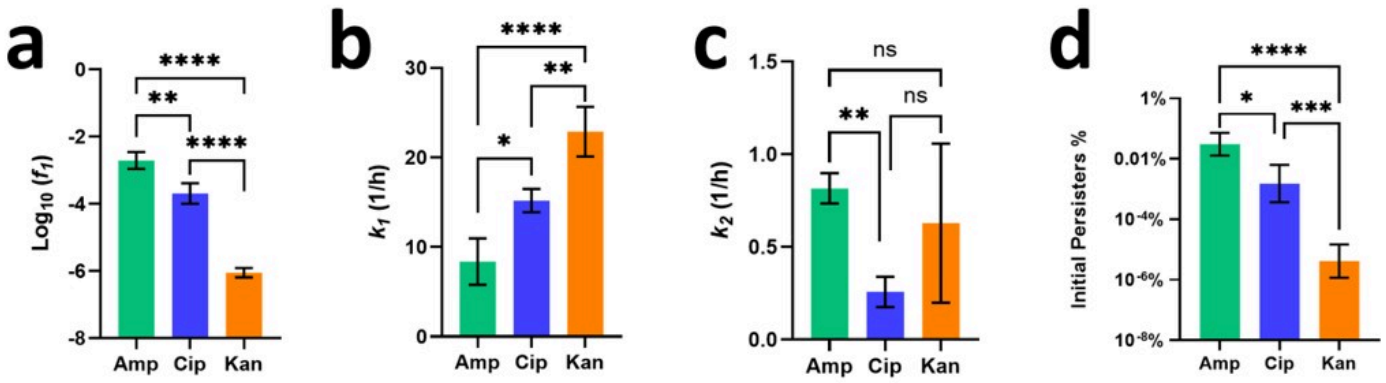


Figure 3

Persister formation and killing kinetics depend on antibiotic types. (a) Persister formation rates vary across antibiotics. Amp: ampicillin; Cip: ciprofloxacin; Kan: kanamycin. (b) Susceptible cells are killed with different rate constants (k_1) across three antibiotics. (c) Persisters are killed with distinct rate constants (k_2) across different antibiotics. (d) Pre-existing persister fractions (P_0%) in exponential-phase cultures before exposure to different drugs. Initial persister fractions (P_0%) were calculated by model fitting and are shown for the exponential-phase cultures derived from 1000-fold seed dilutions. Data are presented as means ± SD from at least three independent replicates. **** $p < 0.0001$; *** $p < 0.001$; ** $p < 0.01$; * $P < 0.05$; ns, not significant.

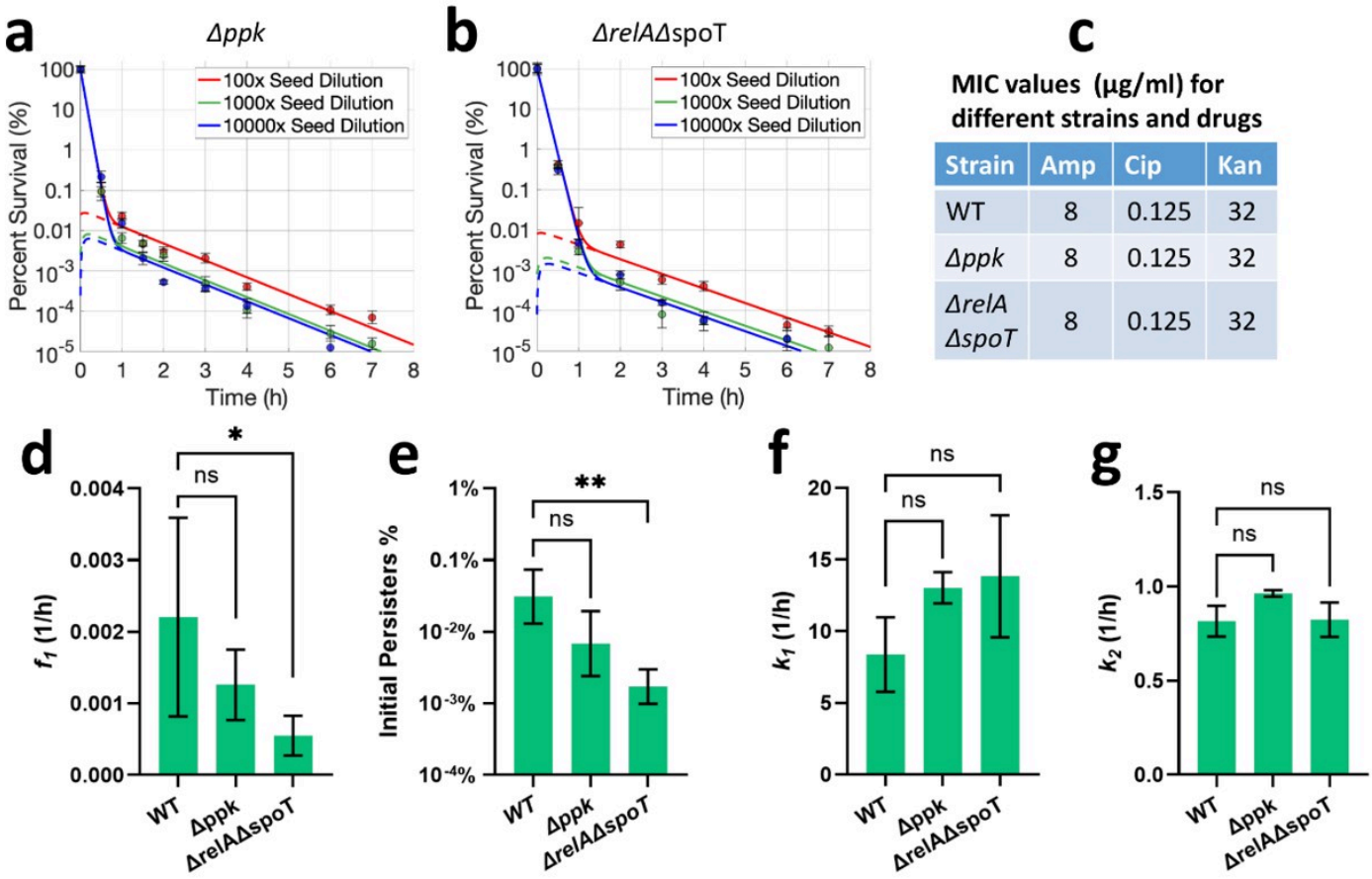


Figure 4

Roles of ppGpp and PPK in persister formation and antibiotic killing. (a, b) SDTK assays for *Δppk*and *ΔrelAΔspoT* strains exposed to ampicillin. *Δppk: gene knockout of polyphosphate kinase gene (ppk); ΔrelAΔspoT: ppGpp null strain.* Representative graphs from four replicates across two independent experiments are shown. Dashed curves represent the persister subpopulation, whereas solid curves represent the total population. (c) No difference in MIC values for wild-type and mutant strains among the antibiotics tested. Amp: ampicillin; Cip: ciprofloxacin; Kan: kanamycin. (d,e) Comparing drug-induced persister formation rates and pre-existing persisters (P_0%) across strains treated with ampicillin. The initial persister fractions were calculated from the exponential-phase cultures seeded from the 1,000-fold dilution. (f,g) Antibiotic killing rates across the wild-type and mutant strains treated with ampicillin. Data are presented with means ± SD with at least three independent experiments. ** $p < 0.01$; * $p < 0.05$; ns, not significant.

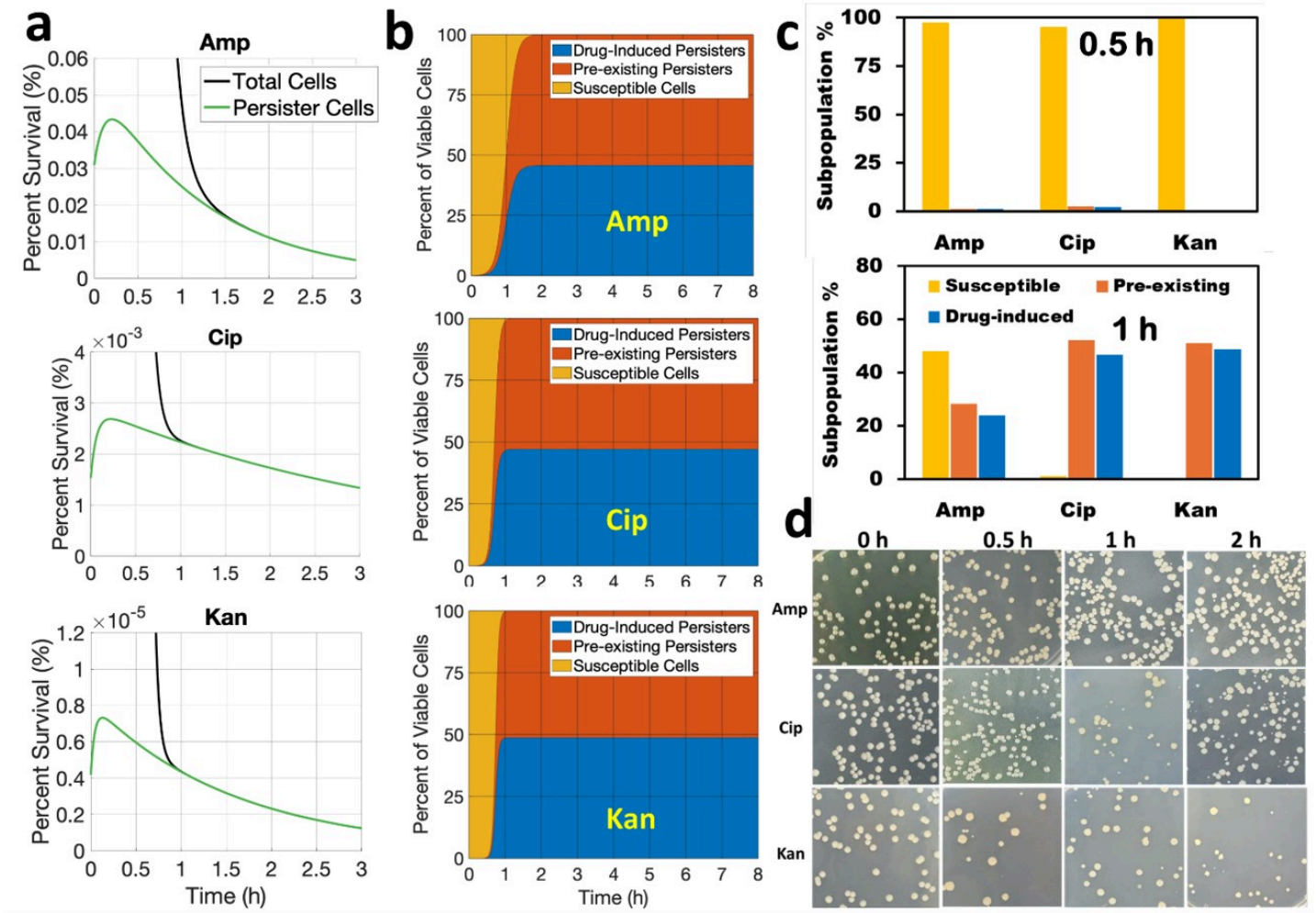


Figure 5

Dynamics of persister formation during antibiotic exposure. (a) Time-resolved dynamics of total population and persister subpopulations during antibiotic exposure in cultures grown from 1,000-fold diluted inocula, revealing rapid drug-induced persister formation. (b) Relative composition of susceptible cells, pre-existing persisters, and drug-induced persisters throughout the course of treatment. Note that the absolute numbers of surviving cells are markedly different across antibiotics. Simulations performed using the mean parameters presented in Fig. 3. (c) Relative fractions of susceptible cells, pre-existing persisters, and drug-induced persisters at 0.5 h and 1 h, extracted from model simulations shown in panel (b). (d)Appearance of small colonies after extended incubation, reflecting prolonged lag times and cellular damage following drug exposure.

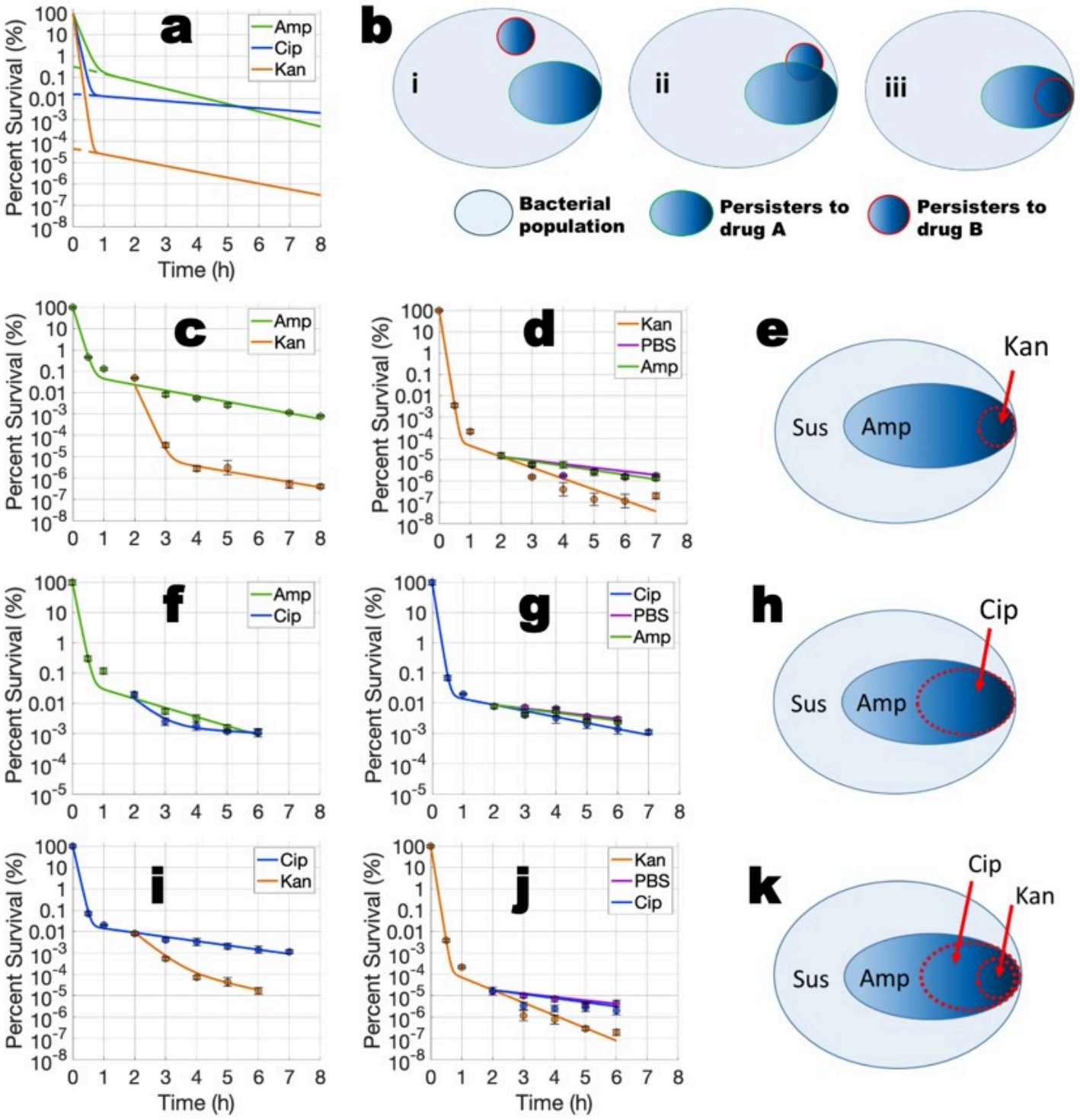


Figure 6

Nested hierarchical relationships and the spectrum of antibiotic persistence revealed by sequential antibiotic treatments. (a) Simulated dynamics of a bacterial culture exposed to ampicillin (Amp), ciprofloxacin (Cip) or kanamycin (Kan) using the averaged parameters measured from this work. Cultures from 100-fold seed dilution were chosen for experiments and simulations because the effect of drug induction on the total persister pool is minimized under this dilution. (b) Graphic demonstration of

the possible relationships between two persister subpopulations: (i) Two distinct subsets, (ii) Two partially overlapping subsets, (iii) One subset embedded within another subset. (c) Exponential-phase cultures were first treated with Amp for 2 h, followed by exposure to either Kan or Amp after removal of the primary drug. (d) Cultures were first treated with Kan, followed by exposure to either Amp, Kan, or PBS after removal of the primary drug. PBS buffer was used as a negative control. (e) Proposed distribution and nested hierarchical relationship between the subsets of ampicillin persisters and kanamycin persisters. Susceptible cells (Sus), ampicillin persisters (Amp), and kanamycin persisters (Kan). (f) Cultures were first treated with Amp, followed by exposure to either Cip or Amp after removal of the primary drug. (g) Cultures were first treated with Cip, followed by exposure to either Amp, Cip, or PBS after removal of the primary drug. (h) Proposed distribution and nested hierarchical relationship between the subsets of ampicillin persisters and ciprofloxacin persisters. (i) Cultures were first treated with Cip, followed by exposure to either Cip or Kan after removal of the primary drug. (j) Cultures were first treated with Kan, followed by exposure to either Kan, Cip, or PBS after removal of the primary drug. (k) Proposed distribution and nested hierarchical relationship among the subsets of susceptible cells, ampicillin persisters, ciprofloxacin persisters, and kanamycin persisters. All cultures tested here were exponential-phase cultures initiated from a 100× dilution of the inoculum. Data represent means ± SD from four replicates across two independent experiments.

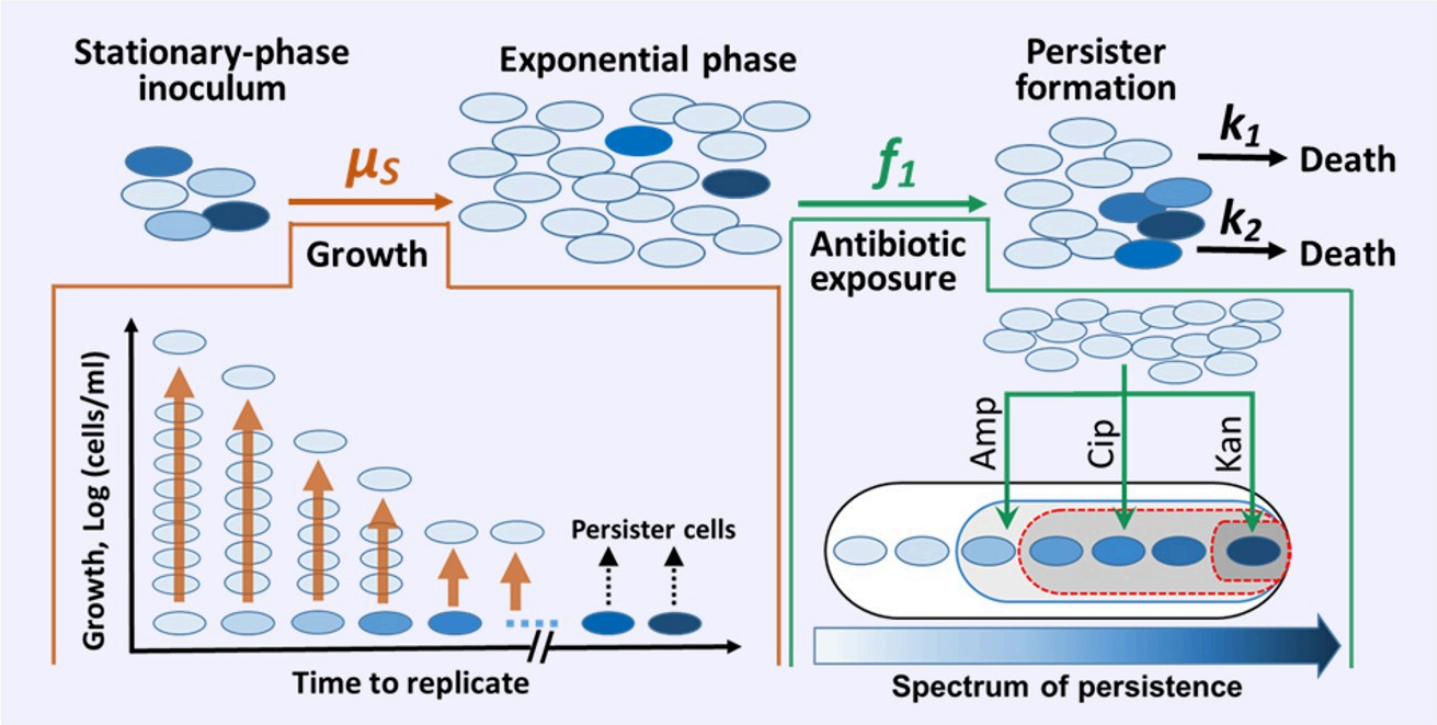


Figure 7

A proposed model for the dynamics of antibiotic persistence. Upon inoculation into fresh medium, most cells rapidly resume growth (light color) and enter the exponential phase, while a small subpopulation, the pre-existing persisters (darker color), remains dormant and tolerant to antibiotics. The revival time of cells follows a power-law distribution, with most cells replicating quickly (light color) and a few

remaining dormant as pre-existing persisters (dark color). The darkness of color denotes the strength of persistence, with darker color indicating higher persistence. During antibiotic exposure, actively growing cells die rapidly (rate constant k_1), whereas a minority activate stress-induced protective responses (e.g., ROS defenses, and/or SOS repair responses) and transition into newly formed persisters (rate constant f_1). Antibiotic persisters are not created equal: different drugs induce different degrees of persistence, and even the same drug can trigger heterogeneity of persistence. Kanamycin selects and generates a small subset of highly persistent cells, while ampicillin selects and induces a relatively weak but large persister pool, with ciprofloxacin's effects being intermediate. Both pre-existing and drug-induced persisters exhibit persistence along a spectrum of tolerance, and can survive or be killed (killing rate constant k_2), depending on whether their repair/recovery capacity overcomes antibiotic-induced damage or not.

Supplementary Files

This is a list of supplementary files associated with this preprint. Click to download.

- SupplementaryInformation.docx